Carbon fibre reinforced poly(vinylidene fluoride): Impact of matrix modification on fibre/polymer adhesion

Michael Q. Tran, Kingsley K.C. Ho, Gerhard Kalinka, Milo S.P. Shaffer, Alexander Bismarck

Accepted Manuscript

Carbon fibre reinforced poly(vinylidene fluoride): Impact of matrix modification on fibre/polymer adhesion

Michael Q. Tran, Kingsley K.C. Ho, Gerhard Kalinka, Milo S.P. Shaffer, Alexander Bismarck

PII: S0266-3538(08)00042-0
DOI: 10.1016/j.compscitech.2008.02.021
Reference: CSTE 3967

To appear in: *Composites Science and Technology*

Received Date: 17 September 2007
Revised Date: 31 January 2008
Accepted Date: 4 February 2008

Please cite this article as: Tran, M.Q., Ho, K.K.C., Kalinka, G., Shaffer, M.S.P., Bismarck, A., Carbon fibre reinforced poly(vinylidene fluoride): Impact of matrix modification on fibre/polymer adhesion, *Composites Science and Technology* (2008), doi: 10.1016/j.compscitech.2008.02.021

Carbon fibre reinforced poly(vinylidene fluoride): Impact of matrix modification on fibre/polymer adhesion

Michael Q. Tran[1], Kingsley K.C. Ho[1], Gerhard Kalinka[2], Milo S.P. Shaffer[3] and Alexander Bismarck[1,*]

[1] Polymer and Composite Engineering (PaCE) Group, Department of Chemical Engineering, Imperial College London, South Kensington Campus, London, SW7 2AZ, UK
[2] Federal Institute for Materials Research and Testing, Division V.6., Unter den Eichen 87, D-12205 Berlin, Germany
[3] Department of Chemistry, Imperial College London, South Kensington Campus, London, SW7 2AZ, UK.

Abstract

The quality of interfacial interaction is dictated by the surface chemistry of the carbon fibres and the composition of the matrix. The composition of poly (vinylidene fluoride) (PVDF) was modified by the addition of maleic anhydride grafted PVDF. The surface properties of the various matrix formulations were characterised by contact angle and electrokinetic measurements. Carbon fibres were modified by industrial electrochemical and oxidation in nitric acid, or the use of a traditional epoxy-sizing of industrially oxidized fibres. The surface composition and morphology and wetting behaviour of the carbon fibres was characterised. The interaction between modified PVDF and the carbon fibres was studied by direct contact angle measurements between PVDF melt on single carbon fibres and by single fibre pull-out tests. The best wetting and adhesion behaviour was achieved between PVDF containing 5 ppm grafted maleic anhydride (MAH) and epoxy-sized carbon fibres. The addition of MAH-grafted PVDF to the unmodified PVDF caused the apparent interfacial shear strength to increase by 184%. The apparent interfacial shear strength of this fibre-matrix combination allowed for the utilisation of 100% of the yield tensile strength of PVDF.

Key words: Carbon fibres, Coupling agents, Interface, Interfacial strength, Adhesion, Wetting

1 Introduction

Polymer matrix composites (PMC) have shown the ability to balance traditional polymer properties such as low part weight and ease of processability with the strength and stiffness of reinforcing agents. Fibre-reinforced thermoplastic composites have become an area of increased interest due to their shorter cycle times and greater potential recycleability compared to thermosetting polymers [1, 2]. Additionally, thermoplastic polymers have long elongations to break which can be particularly beneficial in unidirectional long fibre composites [3]. Carbon fibres are one of the most common reinforcements, however, the nature of the carbon surface

* Corresponding author. Tel.: +44 20 7594 5578; fax: +44 20 7594 5638.
E-mail address: A.Bismarck@imperial.ac.uk (A. Bismarck).

makes fibre-polymer compatibility the largest technical obstacle to widespread use of carbon fibres for a variety of thermoplastic matrices [4, 5].

Fluoropolymers can be found in applications where abrasion, chemical resistance, as well as thermal stability are required. One of the most important fluoropolymers used today is poly (vinylidene difluoride) (PVDF) [6] which is used in a number of applications where chemical resistance, mechanical strength and high creep resistance are required [7]. PVDF is used in piezoelectric sensors, chemically inert pipes and hoses in chemical refineries, wire jacketing for electrical components in areas with possible chemical attack and coatings for skyscraper exteriors [8]. In the off-shore oil and gas industry, PVDF is considered the prime sheathing material for flow, choke and kill lines due to chemical resistance and wide service temperature window (-20°C to 120°C).

When considering the development of composites based on thermoplastics polymers, and more specifically PVDF, it is particularly difficult to ensure good interfacial adhesion between the matrix and the reinforcing fibres [9]. The lack of compatibility between PVDF and many reinforcing agents is due to the inert nature of the matrix and the lack of reactive groups (as compared to thermosetting systems and, indeed, other engineering thermoplastics) which limits the level of interaction between the reinforcement and the matrix. To date, there have only been a few studies that have investigated routes to improve the interaction between fluoropolymers and carbon fibres and these studies have focused only on the effect of fibre surface treatments [9-11]. Two alternative methods for improving the compatibility between carbon fibres and fluoropolymer matrices are the introduction of a miscible secondary polymer into the primary matrix and the modification of the homopolymer with moieties that promote adhesion. PMMA is one of the few polymers miscible in the melt with PVDF [12, 13] but has proven to be ineffective in promoting adhesion to carbon fibres. This paper, therefore, focuses on the use of a modified polymer matrix to interact and/or react with surface functionalities of the carbon fibres which are introduced by conventional surface treatments as a means to ensure adhesion.

Regardless of the route chosen to enhance adhesion, characterising the surface of the individual components provides a better understanding the mechanisms in play. Methods such as contact angle and zeta (ζ) potential measurements have been used to characterise the adhesion behaviour between solids. In addition, the specific interaction between the reinforcing fibre and matrix can be directly quantified by contact angles between polymer melt droplets and individual carbon fibres [14, 15] and single fibre pullout tests [14, 16-18]. Commonly, adhesion is easily be quantified by measuring contact angles (θ) between a solid and a partial wetting liquid. The contact angles of a polymer melt droplet on a fibre can be determined from the shape of a droplet on a fibre using drop length-height methods. This approach has been previously used to determine the interaction between thermoplastics and carbon fibres [19, 20]. Generally it was found that the lower the contact angle, the higher the adhesion is between the matrix and the carbon fibres [20-22].

The quality of interaction between the polymer matrix and fibre reinforcement has long been known to dictate the mechanical performance of the resulting composite. In continuous, unidirectional fibre composites, fibre-matrix interaction has been shown to correlate with interlaminar performance of composite laminates [23]. Single fibre pull out testing provides a means to characterise the interfacial quality of a model single fibre composite [16] while avoiding issues associated with multi-filament, macro-scale composite samples such as degree of impregnation, fibre-fibre interactions and fibre orientation [24]. For a given range of embedded fibre lengths, increases in apparent interfacial shear strength result from improvements in compatibility between the fibre and the matrix resulting from changes to the fibre and/or the matrix, given the embedded lengths of the single fibre are within a modest range [24, 25].

The development of composites based on thermoplastic fluoropolymers is a field that has generated thus far little attention within academia, however, industry seeks materials solutions for applications which require superior chemical resistance and high mechanical strength [26-31]. Carbon fibre reinforced PVDF represents a material, that could be used in applications where chemical resistance and toughness are both required, such as in the (off-shore) oil and gas industry, where currently, conventional monolithic materials are used in deep sea applications but will reach their limit if deeper reservoirs are to be exploited [32, 33].

Since the main factor dictating interfacial adhesion is the composition of the interface which is dependant on both the matrix and fibre surface composition [34], we will investigate the influence of a reactive compatibilising agent for PVDF as a means to improve adhesion to (modified) carbon fibres. The effect of the compatibilising agent on the surface properties of PVDF will be investigated by means of contact angle and ζ-potential measurements. PVDF was blended with various amounts of an reactive compatibiliser (MAH-grafted PVDF) and the adhesion between the matrix and various carbon fibres was quantified by measuring direct contact angles of polymer melt droplets on carbon fibres and single fibre pull out tests to determine the apparent interfacial shear strength (τ_{IFSS}), as measure of practical adhesion.

2 Experimental

2.1 Materials

PVDF (Kynar 711) and maleic anhydride grafted PVDF (MAH-g-PVDF, Kynar ADX-121) were kindly supplied by Arkema (Serquigny, France). Various matrix formulations with increasing MAH-g-PVDF content were prepared by solution precipitation. The PVDF (homopolymer and modified) formulations were dissolved in dimethyl formamide (DMF, general purpose grade, VWR, Poole, UK) to make a 10 wt.-% solution. A non-solvent of 80/20 (wt.-ratio) DMF/water was added drop-wise to induce precipitation. The precipitant was filtered, rinsed with ethanol, and then dried under vacuum at 100°C. The product formed from

solvent precipitation was a fine powder. Samples with the following compositions were prepared: pure PVDF, PVDF containing 1.25 ppm and PVDF containing 5 ppm grafted MAH.

PAN-based carbon fibres with various degrees of surface oxidation with and without sizing were used for this study. Untreated, unsized (C320.000A, CA) and industrially oxidised C320.000B (CB) were kindly supplied by SGL Sigri Carbon (Meitingen, Germany). Severely oxidised carbon fibres were obtained by boiling CA for 5 h in HNO_3 (fuming grade, VWR, Poole, UK) under reflux (T = 120°C). Afterwards, the nitric acid oxidised fibres were washed with distilled water to neutral pH. Commercially-available, industrially-oxidised but unsized AS4 and oxidised AS4 sized with 0.2 wt.-% epoxy-compatible sizing (AS4-GP) were kindly supplied by Hexcel Corporation (Duxford, UK).

2.2 Matrix surface properties

2.2.1 Matrix film preparation

PVDF films with increasing MAH-g-PVDF content were prepared by hot pressing the powder formed after precipitation. The powders were placed directly between two 10 µm Upilex release films and pressed between two polished steel plates at 190°C and 5 MPa of pressure (Moore Presses, Birmingham, UK).

2.2.2 Wetting behaviour of the modified matrix

Contact angles were measured using the Drop Shape Analyser (DSA, Krüss GmbH, Hamburg, Germany) to determine the effect of the changing matrix composition on the wetting behaviour of the PVDF. Two types of contact angles were measured on the pressed films; sessile drop and captive bubble contact angles in order to determine the influence of the surrounding environment on the surface properties of the matrix. Low rate dynamic sessile drop contact angle measurements were performed by placing a droplet of roughly 10 µl of deionised water onto the surface followed by slowly increasing the droplet volume by 10 µl/min. In order to determine the low rate, dynamic, captive bubble, contact angles, the polymer films were equilibrated for 24 h in deionised water to allow polar functional groups to migrate to the surface (a phenomenon called hydrophobic recovery [35, 36]). The contact angles were measured by placing an air bubble of approximately 20 µl below the polymer surface. The bubble volume was increased at a rate of 10 µl/min and the receding contact angle (θ_r), i.e. that of displacing water from the surface, was measured.

2.2.3 Surface character of the modified matrix: ζ-potentials

The Electrokinetic Analyser (EKA, Anton Paar KG, Graz, Austria) based on the streaming potential method was used to determine the ζ-potential of the pressed matrix films. Two films of each matrix formulation were placed parallel to each other in a cell separated by PTFE channel which was 10 mm wide by 75 mm long and 0.5 mm thick. The streaming potential was

measured using two Ag/AgCl electrodes. The system was filled and rinsed with 1 mM KCl electrolyte solution. All entrapped air bubbles were removed at this stage. A pressure drop across the sample (steadily increasing from 30 to 150 mbar) was generated while the electrolyte was pumped through the channel cell. The streaming potential that arose through shear off of the diffuse part of the electrochemical double layer was measured as a function of time and pH at 20°C using two perforated Ag/AgCl electrodes. $\zeta = f(pH)$ was measured starting from natural pH to pH 3 and pH 10, respectively, by adding 0.1 M HCl or 0.1 M KOH by means of an autotitrating unit (RTU, Anton Paar KG, Graz, Austria).

2.3 Carbon Fibre Surface Characterisation

2.3.1 Fibre surface composition

The fibres were characterised by X-ray photoelectron spectroscopy (XPS, ESCA 300, Scienta, Sweden) to determine the level of functionalisation of the modified fibres. An initial survey scan was performed to determine the detectable elements, followed by high resolution scans. An Al K α X-ray source, a slit width of 0.8 mm, and a 90° take off angle was used, which allowed for a spectral resolution of 0.35 eV. The entire X-ray photoelectron spectrum was energy referenced to the C 1s peak of graphite (B.E. = 284.5 eV). After applying the atomic sensitivities for the ESCA 300, peak fitting was performed using a mixed Gaussian-Lorentzian (50/50 mixture ratio) distribution using Casa XPS (version 2.2.60).

2.3.2 Wettability and surface energy of carbon fibres

Contact angles of test liquids on carbon fibres were measured using the modified Wilhelmy-technique. The following test liquids were used; deionised water ($\gamma_l = 72.8$ mN/m), formamide ($\gamma_l = 58.2$ mN/m, 99 % purity, Fisher Scientific) and diiodomethane ($\gamma_l = 50.8$ mN/m, 99 % purity, Fisher Scientific, UK). The advancing (θ_a) and receding (θ_r) contact angles were determined from the mass change *m* during immersion and emersion of the fibres into and from each test liquid using Wilhelmy's equation:

$$\cos\theta = \frac{mg}{\pi \cdot d_f \cdot \gamma_{lv}} \qquad (1)$$

where d_f is the fibre diameter, g is the gravitational acceleration, and γ_{lv} is the surface tension of the test liquid. The surface energy of the carbon fibres γ_f was estimated from the measured contact angles of the test liquids with known surface tension components and parameters using the acid-base approach introduced by van Oss et al. [37]:

$$(1+\cos\theta)\gamma_l = 2(\sqrt{\gamma_s^{LW}\gamma_l^{LW}} + \sqrt{\gamma_s^{+}\gamma_l^{-}} + \sqrt{\gamma_s^{-}\gamma_l^{+}}) \qquad (2)$$

where γ_l is the liquid surface tension, γ^{LW} is the Lifshitz-van der Waals surface tension component of the surface tension, γ^{+} is the Lewis acid parameter of the surface tension, γ^{-} is

the Lewis base parameter of the surface tension and the subscribes s and l denote solid or fibre in our case and liquid. For further details see the following reviews [38, 39]. In order to obtain γ_f of the carbon fibres, which is a sum of the dispersive or Lifshitz/van der Waals component γ_S^{LW} and the acid-base component γ^{AB} ($\gamma^{AB} = 2\sqrt{\gamma_S^- \gamma_S^+}$), contact angles between the fibres and at least 3 different test liquids with known surface energy components and parameters must be measured.

2.3.3 Fibre surface morphology

Fibre surface roughness is known to enhance mechanical interlocking between the fibre and the matrix [34]. Scanning electron microscopy (7 kV, Gemini FEG-SEM, LEO, Germany) was used to determine the surface morphology of the carbon fibres. Samples were prepared by placing the carbon fibres directly on the SEM sample holder using carbon tape. The effect of the various surface treatments on surface roughness was observed.

2.4 Fibre – Matrix Interaction

2.4.1 Wetting behaviour of carbon fibres by polymer melts

The contact angle between polymer melt droplets on single carbon fibres was measured using the generalised length-height method [14]. Individual carbon fibres were attached to a metal frame. The entire metal frame was dipped into polymer powder. The polymer was melted onto the fibres at 220°C in a hot stage (THM600, Linkam Scientific Instruments, Surrey, UK). The polymer melt droplets were imaged using an Olympus BH-2 (Tokyo, Japan) optical microscope. The samples were held at 220°C for 30 min so that the equilibrium droplet shape became established. A total of 50 droplets were imaged on at least three different fibres for each fibre/matrix combination to ensure statistically significant results. Droplet images were imported into a custom made program designed to extract the droplet profile and calculate the contact angle [14].

2.4.2 Single fibre pull-out: Apparent interfacial shear strength (τ_{IFSS})

Single fibre composites for the pull-out tests were prepared by a special embedding machine. This apparatus allows for the production of samples with the fibres orientated perfectly perpendicular to the surface of the matrix at a defined embedded length. A sample of the matrix was heated to the melt on an aluminium sample carrier. The fibre was embedded into the polymer melt droplet at a defined length varying between 50-200 µm [40]. The entire sample was allowed to cool to room temperature in air (approx. 2 min). The fibre diameters were measured using a laser diffraction method [41].

Pull-out experiments were performed on a custom made apparatus which allowed for a short, fibre-free length of 30 µm between the surface of the matrix and fibre-clamping mechanism.

The pull-out tests were performed at a rate of 0.2 µm/s, while recording force and displacement. The maximum load is correlated to the full debonding along the embedded length from the matrix. The shape of the load displacement curve itself reflects on the type failure occurring at the interface [16]. The apparent interfacial shear strength is determined by measuring the force required to debond the embedded fibre from the interface formed with the matrix. For ductile fracture behaviour of the interface, the τ_{IFSS} is independent from the embedded length (L_e) and can be calculated by:

$$\tau_{IFSS} = \frac{F_{max}}{A_e}; \text{ where } \quad A_e = d_f \pi L_e \tag{2}$$

where F_{max} is the maximum force recorded and A_e is the embedded surface area of the fibre.

3 Results and Discussion

3.1 Effect of matrix modification on PDVF surface properties

The effect of incorporating maleic anhydride into PVDF on the wetting behaviour of the matrix was characterised by sessile drop and captive bubble contact angle measurements. Sessile drop measurements probe the wetting behaviour of dry surfaces. In the current case, the advancing sessile drop contact angles (Fig. 1) remained constant with increasing maleic anhydride content, suggesting that the polar functional groups are hidden within the bulk of PVDF film to minimise interfacial energy with the surrounding air [42]. The receding contact angles could not be measured due to pinning of the wetting front of the sessile droplets. Captive bubble contact angles provide a route to measuring receding contact angles but also probe the wetting behaviour of wet surfaces, in contact with a high surface energy medium (γ_{H2O} = 72.8 mN/m); indeed it is known that the polar, MAH, functional groups (or possibly maleic acid if ring opening occurs) can migrate to the surface under such conditions [42]. Thus, the captive bubble contact angle decreases by 10° and 20° upon the addition of 1.25 ppm and 5 ppm of grafted MAH to PVDF, respectively. The measured captive bubble contact angles clearly show the increase in hydrophilicity of the matrix with increasing maleic anhydride content after the polymer surface is in contact with water.

ζ-potentials were measured using the streaming potential method in order to determine the acid-base character of the polymer surfaces. The shape of the ζ-potential curve, as a function of pH, and the low isoelectric point (iep), where ζ = 0 mV, at pH = 3.8, clearly indicates the presence of Brønsted acids on the surfaces of all of the PVDF samples (see Fig. 2). The addition of maleic anhydride/acid does not affect the position of the iep; it remained at pH 3.8. This result suggests that the maleic anhydride/acid functional groups incorporated into the polymer have the same acid strength (pK_a) as the chemical groups naturally present on the surface of the pure PVDF. However, the absolute $\zeta_{plateau}$ value in the high pH region increases with increasing maleic anhydride/acid content, indicating that the concentration of the dissociated acid groups

(likely carboxylic acid groups) is increasing. Thus, the presence of maleic anhydride/acid at the interface is confirmed.

3.2 Surface composition of carbon fibres

Tailoring the surface chemistry of carbon fibres allows for the improvement of adhesion with a matrix by providing sites for possible fibre-matrix interaction. The composition of the carbon fibre surfaces and the identification of the moieties which are generated by the various surface treatments were characterised by XPS. The summary of the surface composition of the carbon fibres used can be found in Table 1. The results from the XPS analysis of the industrially oxidised carbon fibre (CB) show an increase in both the oxygen and nitrogen content as compared to the untreated fibre (CA). The amount of oxygen and nitrogen increased with increasing severity of the oxidation procedure from industrial electrochemical to oxidation in boiling HNO_3. Although, a portion of the nitrogen content on the fibres was attributed to the PAN precursor, nitric acid reflux caused a small but significant increase in the nitrogen containing species on the surface of the carbon fibres. The electrochemically oxidised AS4 and AS4-GP sized with epoxy were also characterised. The relatively high oxygen content of AS4, as compared to sample CB, is likely due to either a more aggressive electrochemical oxidation used by the manufacturer or the fact that AS4 is more susceptible to oxidations. The oxygen content of AS4-GP is due to the uncured epoxy sizing applied to the fibre surfaces. The lack of detectable nitrogen suggests the sizing is masking the nitrogen on the surface of the fibres.

The deconvolution of the high resolution spectra of the major elements present (C 1s, O 1s and N 1s) on the carbon fibres provides information about the chemical environments (or oxidation state) of the elements present on their surfaces. Overlap between the binding energies relating to carbon-oxygen and carbon-nitrogen binds prevents an unambiguous assignment of the chemical environments, due to the similarities between carbon and oxygen and carbon-nitrogen bonds [43]. The resulting deconvoluted peak assignment for the C 1s (Fig. 3A) of the carbon fibre samples exhibited overlap between the C-O and C-N at B.E. = 284.7 eV and C=O and C-N-C at 285.8 eV, similar to previously reported values [43]. Assignment of the deconvoluted curves to potential functional species for the O 1s and N 1s peaks are shown in Fig. 3B and 3C, respectively. For CA, CB and CA-OX three oxygen environments at 531.2 eV, 533.0 eV and 535.7 eV can be distinguished. These peaks were assigned to carbonyl, carbon-oxygen single bond and chemisorbed water, respectively [44]. The N 1s peak deconvolution also shows a number of different chemical environments that include pyridine-N-oxides, pyrrolic and chemisorbed nitroxides at 399.6 eV, 401.4 eV and 405.5 eV, respectively [43]. The oxidation in HNO_3 leads to significant changes in the type of bonded nitrogen. New features appeared at 405.5 eV and 399.6 eV. The new N-species at 405.5 eV can be assigned to $–NO_2$ functionalities and are only found after HNO_3 oxidation [45]. The broad band at 398.8 eV related to C-N species is believed to be pyridine-like rings near graphitic structures [46]. The deconvolution of

the O 1s and N 1s peaks confirms that the surface treatments created a large variety of functional groups.

The introduction of polar oxygen groups onto the surface of the fibres leads to an increase of the fibre surface energy as well as changes to the surface energy components [47]. These groups should lead to improved interaction between the fibre and the modified matrix. At the very least, the increase in the carbon fibre surface energy should lead to better wettability of the fibres by the non-polar matrix (analogous to a Zisman-Neumann plot [48-50]) and, therefore, to a more intimate contact between the phases.

For the contact angles measured using the modified-Wilhemy method, a trend of decreasing contact angles with increasing surface oxygen content was observed for the polar test liquids (water and formamide) for CA, CB and CA-OX as well as for AS4 and AS4-GP fibres. However, AS4 and AS4-GP were observed to be more hydrophobic than CA, CB and CA-OX although they contained more oxygen and nitrogen functional groups. Probing the acid character of the fibre surface with formamide, a Lewis base (γ^+ = 2.3 mN/m, γ^- = 39.6 mN/m) [51], the contact angles for AS4 and AS4-GP were also higher than the CA, CB and CA-OX. The wetting behaviour of the various carbon fibres with diiodomethane, a non-polar surface probe, resulted in contact angles which were again significantly higher for AS4 and AS4-GP than CA, CB and CA-OX. The reason for the differences in the measured contact angles is likely due to differences in graphitic surface structure of the fibres. The precise figures are shown in Table 1. The determination of the surface energy and components added further insight into the wetting behaviour of the fibres.

The overall surface energy of the fibre was determined from the measured contact angles using the acid-base approach (Table 1). The untreated CA fibres had a surface energy of 42.4 mN/m. As expected the increase in polar surface functional groups caused either by industrial (CB) or by HNO_3 oxidation (CA-OX) cause γ_f to increase. This increase is directly proportional to the oxygen content on the fibre surface. Although AS4-GP was sized, the γ_f was identical to that of AS4. For CA, CB and CA-OX γ^{LW} remained constant, whereas γ^{AB} increased with increasing degree of surface functionalisation. Although γ^{AB} for both AS4 and AS-GP was roughly equivalent to that of CB, the γ^{LW} for AS4 and AS4-GP was lower than CA carbon fibres, which again reflects differences in the surface graphitic structure between these two groups of fibres. Although, the Lewis acid (γ^+) and base (γ^-) parameters show that fibres CA, CB and CA-OX have a Lewis basic character, the ratio between γ^+/γ^- increases with increasing oxidation severity. This suggests the oxidation produces a relatively more acidic carbon fibre surface. The surfaces of AS4 and AS4-GP have an amphoteric character.

In addition to surface chemistry, the surface morphology also plays a role in the interfacial adhesion. Rough fibre surfaces provide a means for mechanical interlocking with the matrix. There were two distinct carbon fibre morphologies observed in the SEM (Fig. 4). CA, CB and CA-OX (Fig. 4A-C) have a rough surface topography. The crenalations which are seen in CA

and CB are typical of PAN based fibres which have a lower degree of post carbonisation treatment. Some evidence of surface erosion from acid reflux was apparent in CA-OX (Fig. 4 C). AS4 and AS4-GP (Fig 4D, E) have significantly smoother surfaces than the (oxidised) CA carbon fibres. This difference is likely due to the fibre manufacturing process.

3.3 Adhesion behaviour between carbon fibres and PVDF

The assortment of functional groups on the surface of the carbon fibres is not expected to result in any improved the interaction with pure PVDF [21]. However, some of the functional present on the carbon fibres should favourably interact with the MAH in MAH-g-PVDF. With the exception of carboxyl groups, typical solid carbon oxides, such as carbonyl, phenol, lactol and lactones, are not especially reactive. Since MAH opens to a dicarboxylic acid, hydrogen-bonding may be an option for improved adhesion.

Measuring the direct wetting contact angles between carbon fibre and polymer melt droplets allows for the quantification of the interaction between matrix and carbon fibres. The matrix droplets on the fibres are formed in a dewetting or receding motion and are therefore expected to reflect the higher energetic interaction of the fibre surface [52]. The influence of the MAH-g-PVDF content on the wettability of the carbon fibres is shown in Fig. 5. The PVDF melt contact angle on all unsized fibres (CA, CB, CA-OX and AS4) remains constant, within error, with increasing MAH-g-PVDF content in the matrix. Fig. 6A shows a typical wetting droplet formed between AS4 and PVDF. At higher magnification (Fig. 6B), the bare carbon fibre surface directly adjacent to the wetting droplet is clearly seen. Only clam shell droplets form (Fig. 6C) between AS4 and PVDF containing 5 ppm grafted MAH moieties; making it impossible to determine the contact angle. The observation of this type of droplet shape suggests either this fibre-matrix combination exhibits extremely poor wetting behaviour or that the matrix droplet wetting front is pinned chemically to the fibre surface. On the other hand, unlike the other fibres, the wetting behaviour of AS4-GP appears to improve with the introduction of 1.25ppm MAH-g-PVDF (Fig. 5), with the direct wetting contact angle decreasing to 16° from 22° for pure PVDF. In the case of PVDF containing 5 ppm grafted MAH, it appears that the fibre is completely coated by the polymer (see Fig. 6D). The contact angle for this fibre-matrix formulation could not be determined because the polymer did not dewet the fibre surface to form discrete wetting droplets. This effect is more apparent at higher magnifications as the carbon fibre surface does not show the distinct bare fibre surface observed in Fig. 6B for the CA/PVDF combination. The measurement of the apparent interfacial shear strength provides more information on the quality of the interface between the fibre and the modified matrix.

The failure characteristics of the fibre-matrix interface in single fibre tests were determined by plotting the apparent interfacial shear stress of the pullout tests against the embedded length of the corresponding carbon fibre (Fig. 7). The independence of τ_{IFSS} on the embedded length confirms ductile failure mode of the single fibre composites. The interfacial shear strength

performance, as a function of the maleic anhydride content, can be seen in Fig. 8. τ_{IFSS} for CA in pure PVDF was 15.3 ± 1.2 MPa. The single fibre pull-out testing for CA, CB, CA-OX and AS4 did not show any improvement in interfacial adhesion with increasing MAH-g-PVDF content, a result that is consistent with the direct contact angle measurements. It is clear from these results that conventional fibre surface treatments do not produce the appropriate surface groups to improve the interaction with the maleic anhydride moieties in the modified PVDF matrices.

On the other hand, as shown by the direct wetting, AS4-GP was completely encased by PVDF containing 5 ppm of grafted MAH; therefore, we should expect an increase in practical adhesion. Indeed, with increasing MAH-g-PVDF content, τ_{IFSS} increased from 17.5 ± 2.0 MPa for the pure PVDF to 29.1 ± 2.8 MPa for PVDF containing 1.25 ppm grafted MAH and 44.7 ± 8.2 MPa for PVDF containing 5 ppm grafted MAH, corresponding to a 180% increase over AS4 and pure PVDF ($\tau_{IFSS,\ AS4/PVDF}$ = 15.8 ± 1.6 MPa) fibre-matrix combination. The maximum possible interfacial shear strength is approximately the yield tensile strength of PVDF, in this case, the manufacturer's claims 44.1 - 55.2 MPa. Thus the measured interfacial shear strength suggests that approximately 80 to 100% of the matrix properties can be utilised in a composite. This large increase in τ_{IFSS} can be attributed to a grafting reaction between the epoxide in the sizing on the surface of the AS4-GP and MAH in MAH-g-PVDF.

Even though the scatter is large, the interfacial shear strength correlates with the direct wetting contact angle data; i.e. the smaller the matrix melt wetting contact angle with the fibre, the larger the apparent interfacial shear strength (Fig. 9). The large scatter can be attributed to difficulties in determining such contact angles (i.e. the formation of droplets from a receding motion).

It is commonly assumed that increasing the surface energy of the substrate will result in an improved wetting behaviour by non-polar liquids, such as a PVDF melt (see Zisman or Neumann wetting plots). However, we find that increasing the surface energy of the carbon fibres alone is not sufficient in improving the wetting behaviour, and therefore the interfacial adhesion, of the fibres with PVDF. Having a combination of an appropriate fibre surface treatment and matrix formulation that allows direct chemical reaction is far more effective for the development of carbon fibre reinforced PVDF composites with a sufficient interfacial adhesion.

4 Conclusions

Two methods of improving the interfacial interaction between carbon fibres and PVDF were investigated; the modification of the matrix by adding the compatibilising agent MAH-g-PVDF and functionalisation of the carbon fibre surfaces. Unlike dry, sessile measurements, captive bubble contact angles decreased with increasing maleic anhydride content, highlighting the importance of the interface composition when analysing interfacial interaction. ζ-potentials measured as a function of pH on modified PVDF showed that the acidity (pK_a) of the surface

groups present did not change. However, the concentration of the acidic groups increased with increasing maleic anhydride content.

The carbon fibres investigated were a range of commercial fibres, both untreated and oxidised. As expected with increasing severity of oxidation, the surface oxygen and nitrogen content increases, leading to a rise in overall surface energy of the fibres. Direct contact angle measurements between single fibres and PVDF melt and single fibre pull-out testing provide a means of assessing likely performance in a potential composite, due to differences in surface chemistry and roughness of the fibres and compositional changes within the PVDF matrix. Although, industrial and nitric acid oxidation were effective in increasing the surface energy, neither led to an improved wetting of these fibres by (MAH-g-PVDF modified) PVDF melts nor increased apparent interfacial shear strength of the fibres by the (modified) PVDF.

On the other hand, the wetting behaviour of the epoxy-sized oxidised AS4 (AS4-GP) and PVDF containing 5 ppm grafted MAH indicated complete wetting. The apparent interfacial shear strength of this fibre/matrix combination was 44.7 ± 8.2 MPa; an increase of 155% increase over the same fibre in unmodified PVDF. This fibre-matrix combination allows for almost full utilisation of the intrinsic matrix properties, an unprecedented advancement in carbon fibre fluoropolymer composites.

Acknowledgments

We gratefully acknowledge Arkema and Total, S.A. Group for providing funding for this work. Finally, we would like to acknowledge STFC Daresbury Laboratory, National Centre for Electron Spectroscopy and Surface Analysis for the support for the XPS analysis and Dr. G. Beamson (STFC) for the technical assistance and most valuable comments analysing the XPS data.

References

[1] Henshaw JM, Han WJ, Owens AD. An overview of recycling issues for composite materials. J Thermoplast Compos Mater 1996 (1): 4-20.

[2] Ramakrishna S, Tan WK, Teoh SH, Lai MO. Recycling of carbon fiber PEEK composites. Polymer Blends and Polymer Composites. Clausthal Zellerfeld: Trans Tech Publications 1998:1-8.

[3] Svensson N, Shishoo R, Gilchrist M. Manufacturing of thermoplastic composites from commingled yarns - A review. J Thermoplast Compos Mater 1998; 11:22-56.

[4] Park SJ, Papirer E, Donnet JB. Influence of Electrochemical Treatment on the Surface-Properties of Carbon-Fibers - Acid-Base Character and Adsorption Enthalpy. J Chim Phys Phys-Chim Biol 1994;91:203-222.

[5] Morgan P. Carbon fibres and their composites. New York: CRC Press 2005.

[6] Priya L, Jog JP. Poly(vinylidene fluoride)/clay nanocomposites prepared by melt intercalation: Crystallization and dynamic mechanical behavior studies. J Polym Sci B 2002; 40(15):1682-1689.

[7] Drobny JG. Blends and composites based on fluoropolymers. Macromol Symp 2001;170:149-156.

[8] Humphrey J, Amin-Sanayei R. Vinylidene Fluoride Polymers. In: Mark H, ed. Encyclopedia of Polymer Science and Technology. 3 ed. New York: Wiley 2003.
[9] Bismarck A, Schulz E. Adhesion and friction behavior between fluorinated carbon fibers and poly (vinylidene fluoride). J Mater Sci 2003;38:4965-4972.
[10] Kostov GK, Nikolov AT. Carbon-Fiber Modified Composites of Tetrafluoroethylene-Ethylene Copolymers. Polym. Composites 1994;15:367-374.
[11] Park SJ, Seo MK, Rhee KY. Studies on mechanical interfacial properties of oxy-flourinated carbon fibers-reinforced composites. Mater Sci Eng A 2003;356:219-226.
[12] Moussaif N, Marechal P, Jerome R. Ability of PMMA to Improve the PC/PVDF Interfacial Adhesion. Macromol. 1997;30:658-659.
[13] Andrews JRF, Bevis M. The butt-fusion welding of PVDF and its composites. J Mater Sci 1984;19:653-671.
[14] Song BH, Bismarck A, Tahhan R, Springer J. A generalized drop length-height method for determination of contact angle in drop-on-fiber systems. J Colloid Interface Sci 1998;197:68-77.
[15] Song B, Bismarck A, Springer J. Contact Angle Measurements on Fibers and Fiber Assemblies, Bundles, Fabrics, and Textiles. In: Hartland S, ed. Surface and Interface Tension: Measurement, Theory, and Application. Basel: Marcel Dekker, Inc. 2004:425-481.
[16] DiFrancia C, Ward TC, Claus RO. The single-fibre pull-out test 1. Review and interpretation. Compos A 1996;27:597-612.
[17] Favre JP, Desarmot G, Sigety P. Fibre/polymer tests at the fibre scale: Tools for analysing and optimizing the composite response to mechanical loads. In: Interfacial Effects in Particulate, Fibrous and Layered Composite Materials. Clausthal Zellerfeld: Trans Tech Publications 1996:133-152.
[18] Zhou LM, Mai YW, Baillie C. Interfacial Debonding and Fiber Pull-out Stresses 5. A Methodology for Evaluation of Interfacial Properties. J Mater Sci 1994;29:5541-5550.
[19] Bismarck A, Richter D, Wuertz C, Springer J. Basic and acidic surface oxides on carbon fiber and their influence on the expected adhesion to polyamide. Colloids Surf A 1999;159:341.
[20] Bismarck A, Richter D, Wuertz C, Kumru ME, Song B, Springer J. Adhesion: Comparison between physico-chemical expected and measured adhesion of oxygen-plasma-treated carbon fibers and polycarbonate. J Adhesion 2000;73:19-42.
[21] Ho KKC, Kalinka G, Tran MQ, Polyakova NV, A. B. Fluorinated carbon fibres and their suitability as reinforcement for fluoropolymers. Compos Sci Technol 2007;67:2699-2706.
[22] Ho KKC, Lamoriniere S, Kalinka G, Schulz E, Bismarck A. Interfacial behaviour between atmospheric plasma fluorinated carbon fibres and poly (vinylidene fluoride). J Colloid Interface Sci 2007;313: 476–484.
[23] Park SJ, Kim MH. Effect of acidic anode treatment on carbon fibers for increasing fiber-matrix adhesion and its relationship to interlaminar shear strength of composites. J Mater Sci 2000;35:1901-1905.
[24] Pisanova E, Zhandarov S. Fiber-Reinforced Heterogeneous Composites (HCs). In: Brostow W, ed. Performance of Plastics. Cincinnati: Hanser Gardner 2000:461-86.
[25] Piggott MR. Why interface testing by single-fibre methods can be misleading. Compos Sci Tech 1997;57:965-974.
[26] Lee JC, Suzuki N, Kondo S, Sato H, inventors; Mitsui Du Pont Fluorochemical [JP];Du Pont [US], assignee. Fluororesin Composite Compositions. JP 1598396 (A1). 2005.
[27] Marena A, inventor Teleflex Fluid Systems (Suffield, CT), assignee. Composite hose assembly. US 6,257,280. 2001.
[28] Blasko DS, Fisher WC, Swails MR, inventors; Parker-Hannifin Corporation (Cleveland, OH), assignee. Tubular polymeric composites for tubing and hose constructions. US 6,776,195. 2002.
[29] Oshima A, Udagawa A, Morita Y, Seguchi T, Tabata Y, inventors; Japan Atomic Energy Research Institute (Tokyo, JP), assignee. Fluoroplastic composites and a process for producing the same. JP 6,204,301. 2001.
[30] Ueno T, Inamori M, inventors; Osaka Gas Company, Limited (Osaka, JP), assignee. Method of producing graphite fiber-reinforced fluororesin composites. JP 5,705,120. 1998.

[31] Driggett RA, Scott WC, inventors; Tox-Wastech, Inc. (Wheaton, IL), assignee. High Strength composite materials. US 5,902,755. 1999.
[32] Black S. Composites alive and well in offshore oil applications. High Perform Compos 2006 2006.
[33] Wang SS. Composites key to deepwater oil & gas. High Perform Compos. 2006.
[34] Tang LG, Kardos JL. A review of methods for improving the interfacial adhesion between carbon fiber and polymer matrix. Polym Compos. 1997;18:100-113.
[35] Garbassi F, Morra M, Occhiello E. Polymer surfaces: From Physics to Technology. Chichester: Wiley 1998.
[36] Garbassi F, Occhiello E. Surfaces and Their Modification. In: Brostow W, ed. Performance of Plastics. Cincinnati: Hanser Gardner 2000:373-400.
[37] Della Volpe C, Maniglio D, Brugnara M, Siboni S, Morra M. The solid surface free energy calculation - I. In defense of the multicomponent approach. J Colloid Interface Sci 2004; 271: 434-453.
[38] Good RJ. Contact Angle, Wetting, and Adhesion - A Critical Review. J Adhes Sci Technol 1992;6:1269-1302.
[39] Kwok DY, Neumann AW. Contact angle measurement and contact angle interpretation. Adv Colloid Interface Sci 1999;81:167-249.
[40] Hampe A, Boro I, Schuhmacher K. Bestimmung der Haftung zwischen Faser und Matrix. Forschung Aktuell der TU Berlin 1990;7:21-23.
[41] Meretz S, Linke T, Schulz E, Hampe A, Hentschel M. Diameter measurement of small fibres: laser diffraction and scanning electron microscopy technique results do not differ systematically. J Mater Sci Lett. 1992;11:1471-1472.
[42] Ko YC, Ratner BD, Hoffman AS. Characterization of Hydrophilic-Hydrophobic Polymeric Surfaces by Contact-Angle Measurements. J Colloid Interface Sci 1981;82:25-37.
[43] Biniak S, Szymanski G, Siedlewski J, Swiatkowski A. The characterization of activated carbons with oxygen and nitrogen surface groups. Carbon 1997;35(12):1799-1810.
[44] Lee WH, Lee JG, Reucroft PJ. XPS study of carbon fiber surfaces treated by thermal oxidation in a gas mixture of O-2/(O-2+N-2). Appl Surf Sci 2001;171:136-142.
[45] Wu ZH, Pittman CU, Gardner SD. Nitric-Acid Oxidation of Carbon-Fibers and the Effects of Subsequent Treatment in Refluxing Aqueous NaOH. Carbon 1995;33:597-605.
[46] Reis MJ, Dorego AMB, Dasilva JDL, Soares MN. An Xps Study of the Fiber-Matrix Interface Using Sized Carbon-Fibers as a Model. J Mater Sci 1995;30:118-126.
[47] Bismarck A, Kumru ME, Song B, Springer J, Moos E, Karger-Kocsis J. Study on surface and mechanical fiber characteristics and their effect on the adhesion properties to a polycarbonate matrix tuned by anodic carbon fiber oxidation. Composites A 1999;30:1351-1366.
[48] Spelt JK, Dongqing L. The Equation of State Approach to Interfacial Tensions. In: Neumann AW, Spelt JK, eds. Applied Surface Thermodynamics. New York: Dekker 1996.
[49] Patterson D, Delmas G. Corresponding States Theories and Liquid Models. Disc Faraday Soc 1970;49:98-105.
[50] Patterson D, Rastogi AK. The Surface Tension of Polyatomic Liquids and the Principle of Corresponding States. J Phys Chem 1970;74:1067-1071.
[51] Erbil HY. Surface tension of polymers. In: Birdi KS, ed. Handbook of surface and colloid chemistry. Boca Raton, Fla.: CRC Press 1997:292.
[52] Wu S. Polymer Interface and Adhesion. New York: Dekker 1982.

Figures List

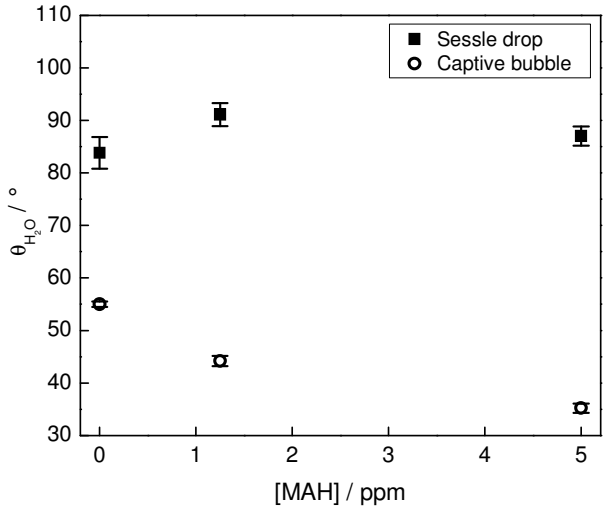

Figure 1. Advancing sessile drop and receding captive bubble contact angles for PVDF, PVDF w/ 1.25 ppm [MAH], and PVDF w/ 5.00 ppm [MAH].

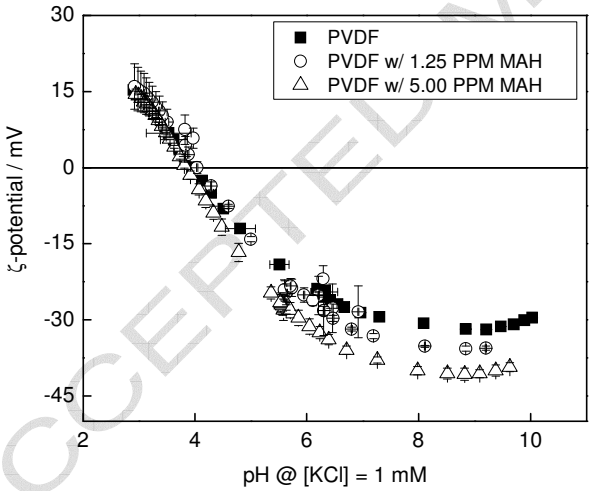

Figure 2. The ζ potential as a function of pH for the matrix formulations in this study.

Table 1. Fibre diameter, surface composition, advancing and receding contact angles versus the various test liquids and calculated surface energy and surface energy components of the carbon fibres studied.

Fibre	d_{fibre} (µm)	C 1s (% at.)	O 1s (% at.)	N 1s (% at.)	Water (θ_a/ θ_r)	Formamide (θ_a/ θ_r)	Diiodomethane (θ_a/ θ_r)	γ^s (mJ/m)	γ^{LW} (mJ/m)	γ^{AB} (mJ/m)	γ^+ (mJ/m)	γ^- (mJ/m)
CA	7.80 ±0.19	95.8	3.4	0.8	76.2 ± 1.2 50.1 ± 1.2	55.7 ± 3.1 43.9 ± 2.2	35.3 ± 3.8 28.0 ± 2.7	42.4 ± 3.6	41.9 ± 1.8	0.6 ± 1.8	0.0 ± 0.1	8.1 ± 1.9
CB	7.92 ±0.12	94.5	4.1	1.3	72.3 ± 0.6 52.6 ± 2.9	44.6 ± 5.1 30.1 ± 3.5	35.3 ± 1.8 29.5 ± 2.1	46.2 ± 3.5	41.9 ± 0.8	4.4 ± 2.7	0.7 ± 0.7	6.6 ± 2.0
CA-OX	7.24 ±0.10	83.7	12.7	3.6	55.9 ± 4.6 40.1 ± 5.0	23.7 ± 2.5 22.6 ± 2.8	39.7 ± 1.8 24.6 ± 2.5	52.3 ± 4.6	39.8 ± 0.9	12.5 ± 3.7	2.8 ± 0.7	14.0 ± 4.8
AS4	7.28 ±0.11	90.6	7.0	2.4	77.2 ± 4.4 56.8 ± 5.7	46.3 ± 2.6 35.9 ± 0.5	59.7 ± 2.9 58.8 ± 0.7	36.1 ± 5.8	28.7 ± 1.7	9.4 ± 4.1	4.1 ± 1.3	3.3 ± 2.7
AS4-GP	7.24 ±0.14	88.5	10.6	--	81.4 ± 4.9 68.4 ± 4.3	49.2 ± 2.1 37.4 ± 2.9	58.0 ± 0.2 57.2 ± 0.1	34.9 ± 3.9	29.7 ± 0.1	5.1 ± 3.8	3.5 ± 1.0	1.9 ± 2.3

A)

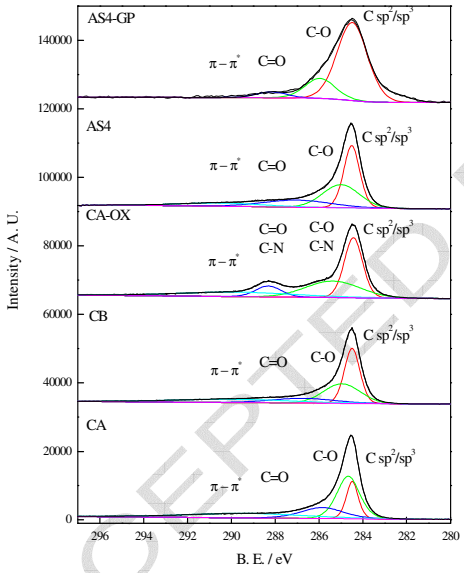

B)

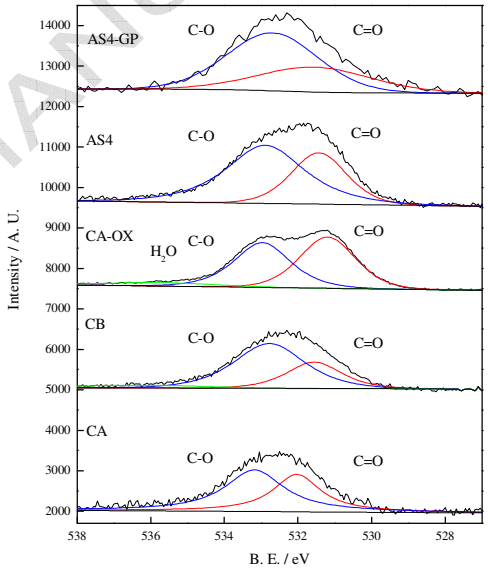

C)

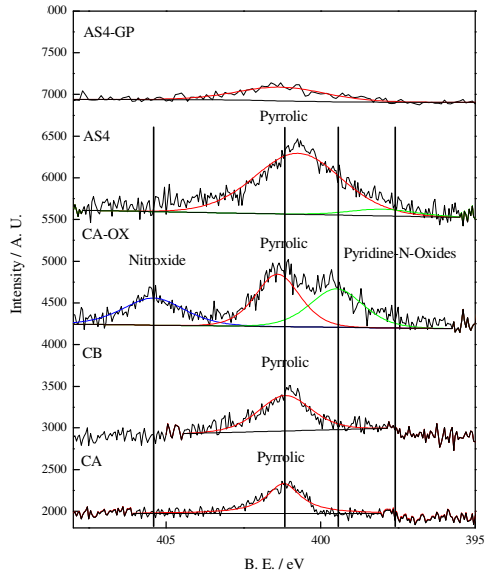

Figure 3. X-ray photoelectron spectra of A) C 1s, B) O 1s, and C) N 1s CA, CB, CA-OX, AS4, and AS4-GP.

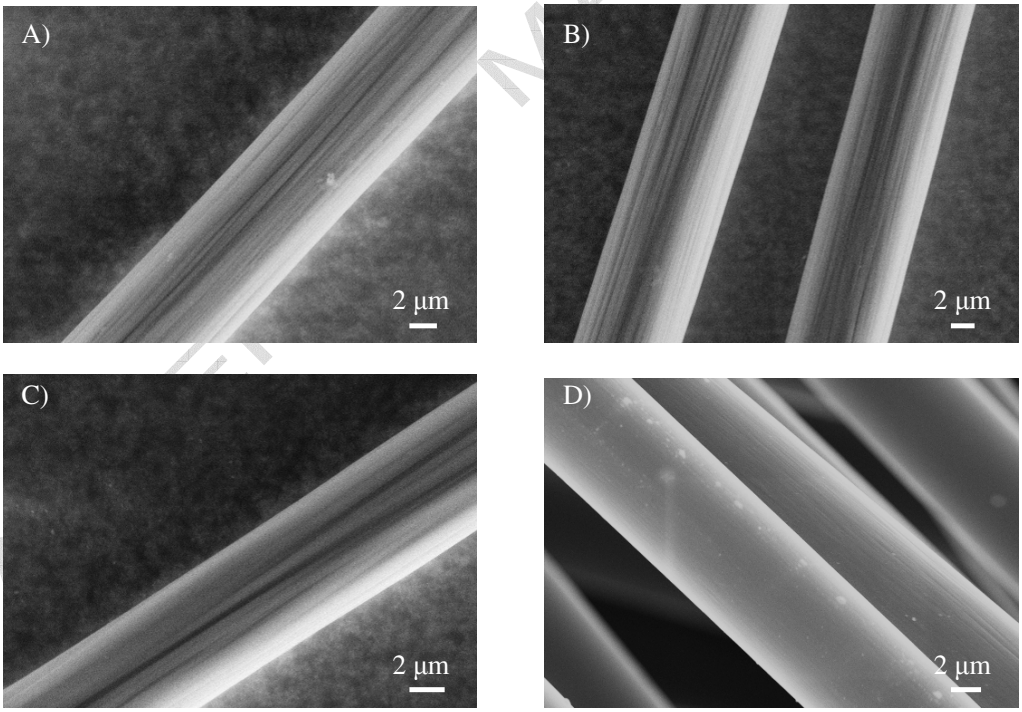

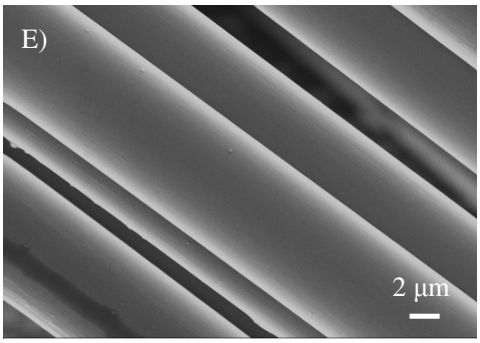

Figure 4. SEM micrographs of the various carbon fibres investigated CA (A), CB (B), CA-OX (C), AS4 (D), and AS4-GP (E).

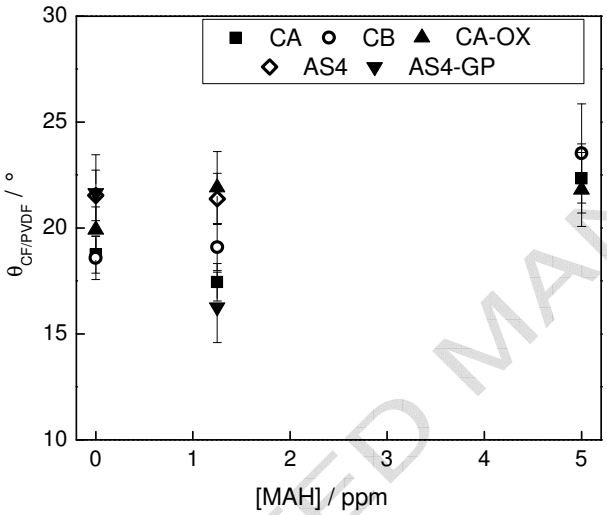

Figure 5. Direct wetting contact angle as a function of [MAH].

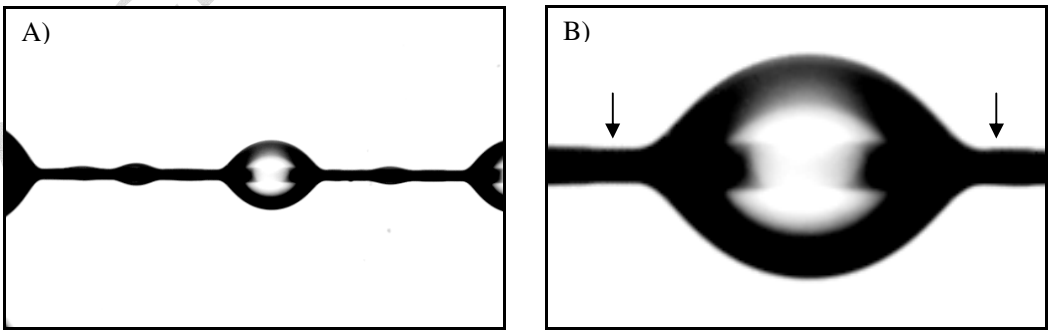

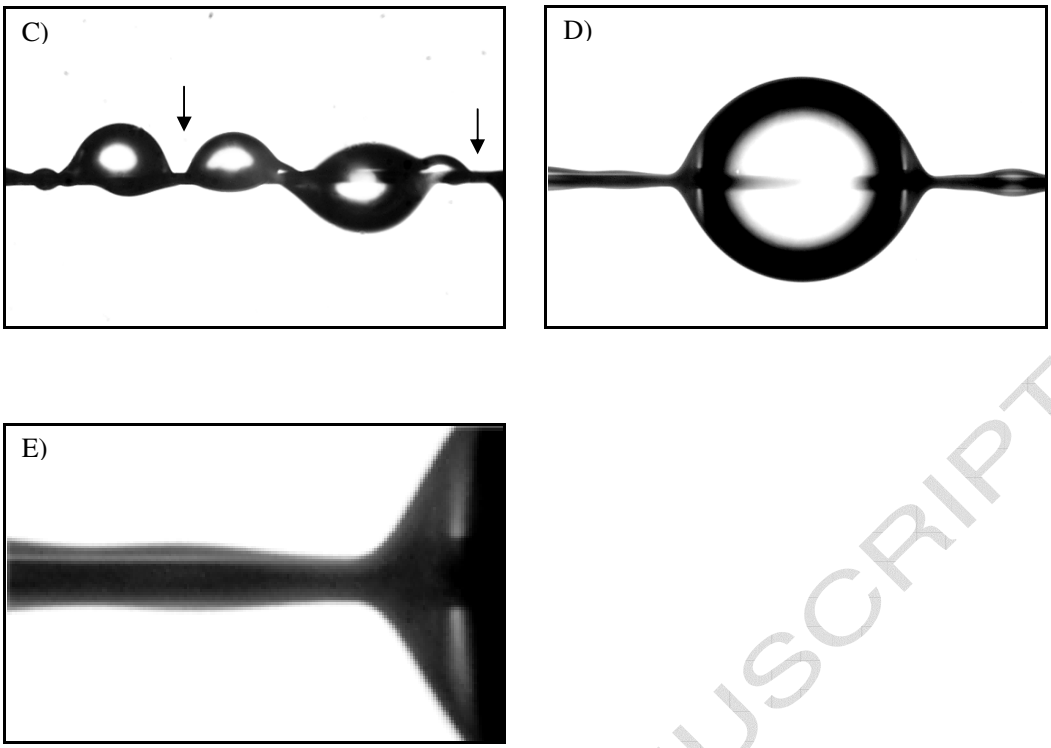

Figure 6. A) Typical droplets on AS4 formed with PVDF. B) Shows a higher magnification of AS4 with a PVDF wetting droplet. Note the distinct bare fibre adjacent to the drop. C) Shows clam shell type droplets formed between [MAH] = 5.00 ppm and AS4. D) Shows a completely polymer encased AS4-GP fibre with [MAH] = 5.00 ppm. E) A higher magnification of the encased AS4-GP fibre with 100% MAH-g-PVDF.

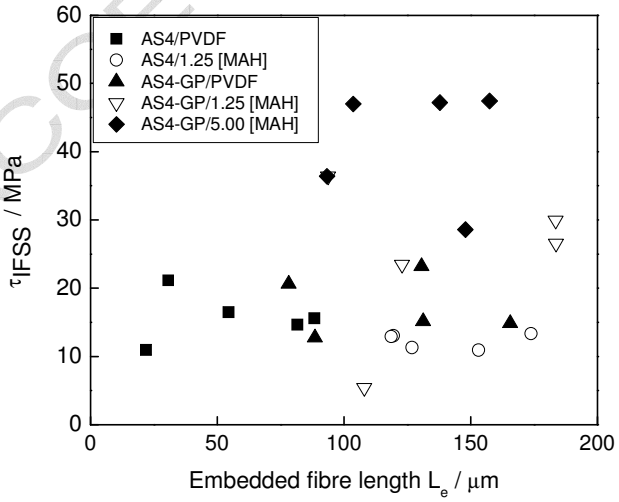

Figure 7. τ_{IFSS} as a function of the embedded length of the fibre for AS4/PVDF; AS4/PVDF w/ 1.25 ppm [MAH]; AS4-GP/PVDF; AS4-GP/PVDF w/ 1.25 ppm [MAH]; and AS4-GP/PVDF w/ 5.00 ppm [MAH].

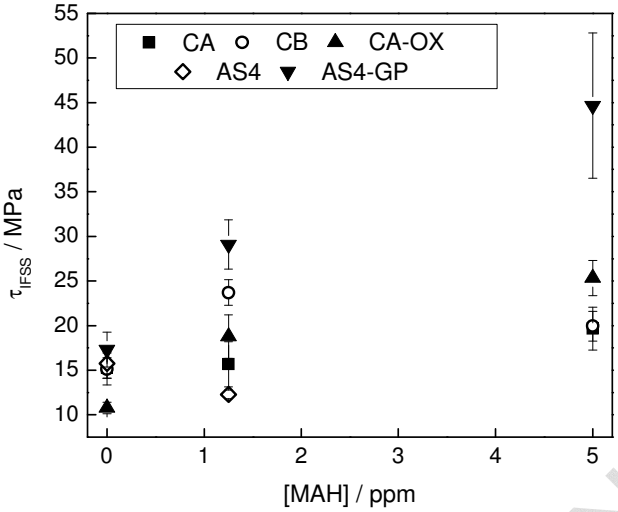

Figure 8. τ_{IFSS} as a function of concentration of MAH in PVDF for untreated, various oxidised fibres used in this study.

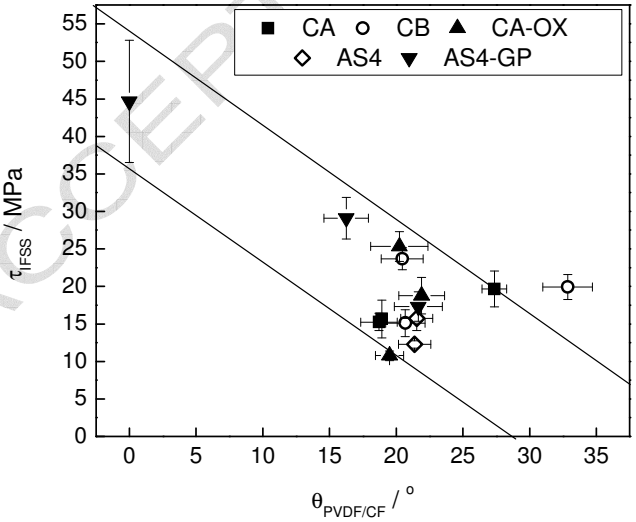

Figure 9. τ_{IFSS} as a function of the contact angle between carbon fibres and PVDF melt.